

# Quantitative estimates of impact induced crustal erosion during accretion and its influence on the Sm/Nd ratio of the Earth

L. Allibert<sup>a,b,\*</sup>, S. Charnoz<sup>a</sup>, J. Siebert<sup>a,e</sup>, S.A. Jacobson<sup>c</sup>, S.N. Raymond<sup>d</sup>

<sup>a</sup>*Institut de Physique du Globe de Paris, Université de Paris, 1 Rue Jussieu, Paris, France*

<sup>b</sup>*Museum für Naturkunde Berlin, Leibniz Institute for Evolution and Biodiversity Science, Invalidenstrasse 43, Berlin 10115, Germany*

<sup>c</sup>*Michigan State University, Earth and Environmental Sciences, 288 Farm Ln, East Lansing, MI 48824, USA*

<sup>d</sup>*Laboratoire d'Astrophysique de Bordeaux, Allée Geoffroy St Hilaire, Bordeaux, France*

<sup>e</sup>*Institut Universitaire de France*

## Abstract

Dynamical scenarios of terrestrial planets formation involve strong perturbations of the inner part of the solar system by the giant-planets, leading to enhanced impact velocities and subsequent collisional erosion. We quantitatively estimate the effect of collisional erosion on the resulting composition of Earth, and estimate how it may provide information on the dynamical context of its formation. The composition of the Bulk Silicate Earth (BSE, Earth's primitive mantle) for refractory and lithophile elements (RLE) should be strictly chondritic as these elements are not affected by volatile loss nor by core formation. However, an excess in  $^{142}\text{Nd}$  compared to the  $^{144}\text{Nd}$  has been emphasized in terrestrial samples compared to most measurements in chondrites. In that case, the Samarium/Neodymium (Sm/Nd) ratio could be roughly 6% higher in the BSE than in chondrites, as suggested from the  $^{146}\text{Sm}/^{142}\text{Nd}$  isotope system (Boyet and Carlson, 2005). This proposed chemical offset could be the consequence of preferential collisional erosion of the crust during the late stages of Earth's accretion, leaving a BSE enriched in Sm due to its lower incompatibility compared to Nd (O'Neill and Palme, 2008; Boujibar et al., 2015; Bonsor et al., 2015; Carter et al., 2015, 2018). However, if the present  $^{142}\text{Nd}$  of the BSE arises from nucleosynthetic heterogeneities within the protoplanetary disk (Burkhardt et al., 2016; Bouvier and Boyet, 2016; Boyet et al., 2018), then the BSE has no excess in Sm compared to Nd and this hypothesis precludes any significant loss of relatively Nd-enriched component early in the Solar System. Here, we simulate and quantify the erosion of Earth's crust in the context of Solar System formation scenarios, including the classical model and Grand Tack scenario that invokes orbital migration of Jupiter during the gaseous disk phase (Walsh et al., 2011; Raymond et al., 2018). We find that collisional erosion of the early crust is unlikely to explain the proposed superchondritic Sm/Nd ratio of the Earth for most simulations. Only Grand Tack simulations in which the last giant impact on Earth occurred later than 50 million years after the start of Solar System formation can account for this Sm/Nd ratio. This time frame is consistent with current cosmochemical and dynamical estimates of the Moon forming impact (Chyba, 1991; Walker, 2009; Touboul et al., 2007, 2009, 2015; Pepin and Porcelli, 2006; Norman et al., 2003; Nyquist et al., 2006; Boyet et al., 2015). However, such a late fractionation in the Sm/Nd ratio is unlikely to be responsible for a 20-ppm  $^{142}\text{Nd}$  excess in terrestrial rocks due to the half life of the radiogenic system. Additionally, such a large and late fractionation in the Sm/Nd ratio would accordingly induce non-observed

---

\*Corresponding author

Email address: [allibert@ipgp.fr](mailto:allibert@ipgp.fr) (L. Allibert)

anomalies in the  $^{143}\text{Nd}/^{144}\text{Nd}$  ratio. Considering our results, the Grand Tack model with a late Moon-forming impact cannot be easily reconciled with the Nd isotopic Earth contents.

---

**Keywords.** Cratering - Planetary Formation - Cosmochemistry - Accretion - Abundances, interiors

## 1. introduction

Chondrites are primitive meteorites that did not differentiate into a core, silicate mantle and crust, and therefore are thought to reflect the chemical compositions of their entire parent bodies. Chondrites have accordingly been considered as the most appropriate proxy for the bulk composition of Earth (Ringwood, 1966; Allègre et al., 1995; Boyet and Carlson, 2005). Whether the Earth building blocks are made of carbonaceous, ordinary or enstatite chondrites, or chondritic at all is still a matter of debate (Warren, 2011; Dauphas, 2017; Drake and Righter, 2002). Notably, considering isotopic compositions, Earth is more similar to enstatite chondrites (e.g. Javoy and Pineau, 1983; Clayton et al., 1984; Cartigny et al., 1997; Dauphas et al., 2004) while considering elemental abundances, carbonaceous chondrites are closest to Earth except for volatile elements (McDonough and Sun, 1995; Halliday, 2013).

Assuming the chondrites represent Earth’s building blocks, the bulk silicate Earth should be in chondritic proportions for refractory and lithophile elements (RLE) as they are neither affected by volatile loss nor core formation (i.e. RLE do not enter metal or sulphide phases). Sm and Nd are considered as RLE that can constitute powerful tracers of collisional erosion because of their geochemical properties (e.g. RLEs, incompatibility degrees, geochronological properties.  $^{146}\text{Sm}$  decays to  $^{142}\text{Nd}$  with a half life of  $\sim 68\text{-}103$  Myr (Kinoshita et al., 2012; Friedman et al., 1966; Meissner et al., 1987). Geochemical studies have enlightened a  $^{142}\text{Nd}/^{144}\text{Nd}$  ratio for terrestrial rocks of roughly 20 ppm (part per million) higher than various types of chondrites (ranging from  $-35\pm 15$  ppm for carbonaceous chondrites to  $-10\pm 12$  ppm for enstatites) (Boyet and Carlson, 2005). This small but significant difference might suggest that the BSE Sm/Nd ratio is  $+6\%$  ( $\pm 1\%$ ) above the average chondritic value (Boyet and Carlson, 2005). However after 68-103 Myr, half of the initial amount of  $^{146}\text{Sm}$  would have decayed already in  $^{142}\text{Nd}$ , implying only half the effect of a  $^{142}\text{Nd}/^{144}\text{Nd}$  fractionation onto the Sm/Nd ratio. Additionally, the 6% excess in Sm/Nd ratio estimate implies that the fractionating process would have occurred within the 30 first millions years of the solar system formation in order to preserve a low fractionation in  $^{143}\text{Nd}/^{144}\text{Nd}$  (Boyet and Carlson, 2005).

A possible explanation to an excess in the Earth Sm/Nd ratio compared to chondrites (Boyet and Carlson, 2005) is that the Earth’s mantle underwent an early fractionation event induced by partial melting during the first few hundred Myr of solar system history. Mojzsis et al. (2019) have shown that extensive crustal melting can still happen after 100 Myr due to late accretion. Nd is enriched in magmas with respect to Sm during melting process, i.e. Nd is more incompatible than Sm (e.g. Workman and Hart, 2005). Thus, an early crust-mantle differentiation can produce an incompatible-elements depleted mantle corresponding to the present BSE as well as an enriched reservoir with low Sm/Nd corresponding to a primitive basaltic reservoir. This missing reservoir could be still hidden in the deep mantle after subduction of the primordial crust or formation of a basal magma ocean at the core mantle boundary (Boyet and Carlson, 2005; Campbell and O’Neill, 2012) that would be unsampled. Another possibility is that this reservoir represents Earth’s early

crust, which was collisionally eroded during the late stages of planetary accretion (O'Neill and Palme, 2008; Campbell and O'Neill, 2012; Boujibar et al., 2015; Bonsor et al., 2015; Carter et al., 2015, 2018; Shibaike et al., 2016), leading to the inferred superchondritic Sm/Nd ratio. Total erosion of crust about 1% – 1.5 of Earth mass may be required to account for the fractionation of the BSE Sm/Nd ratio (O'Neill and Palme, 2008) if Earth's building blocks were made of either ordinary or carbonaceous chondrites. This number is highly dependant on the partial melting rate assumed in the model (O'Neill and Palme, 2008), on the crustal composition (MORB type here) but also on the dependency with the one-impact erosion assumption. Other estimates can be provided considering other evidences. For example, considering the Mg/Si ratio as well as the hypothesis that the Earth building blocks are made of enstatite chondrites, Boujibar et al. (2015) estimate that 15wt% of crust may have to be preferentially removed during accretion. However, the Earth is only showing a 10-ppm deficit (Burkhardt et al., 2016) in  $^{142}\text{Nd}$  relatively to the  $^{144}\text{Nd}$  for enstatite chondrites instead of 20-ppm when considering the average over all chondrites (Boyet and Carlson, 2005) suggesting a lower loss of crust required to account for this deficit.

Additionally, recent studies have shown that the existence of nucleosynthetic anomalies in pristine planetary precursors such as chondrites and Ca-Al rich refractory inclusions (CAIs) could cause the observed variations in the  $^{142}\text{Nd}$  abundances among planetary materials (Burkhardt et al., 2016; Bouvier and Boyet, 2016). Moreover, few CAIs and enstatite chondrites have also been shown recently to share common Nd isotope signatures with terrestrial rocks (Bouvier and Boyet, 2016; Boyet et al., 2018). These observations would imply a chondritic Sm/Nd ratio for the Earth and would preclude dynamical accretion scenarios leading to efficient crustal erosion. However, planetary accretion processes involve energetic impacts with potentially significant erosion of material from embryos (Leinhardt and Stewart, 2011; Leinhardt et al., 2015; Bonsor et al., 2015; Marcus et al., 2009). Thus, it is necessary to quantify the efficiency of collisional erosion of the primordial crust to address the issue of Earth's accretion scenario and the nature of its building blocks. In previous studies, the efficiency of this process has been investigated with either a simple erosion model (Shibaike et al., 2016) focusing only on the period of the terminal lunar cataclysm (TLC), the existence of which is in question (Boehnke and Harrison, 2016; Zellner, 2017; Morbidelli et al., 2018; Hartmann, 2019; Mojzsis et al., 2019) or neglecting the effect of a population of small planetesimals (Carter et al., 2018). Notably, Shibaike et al. (2016) showed that the eventual TLC would not be responsible for removing the entire Hadean crust but most of it. These are estimations based on excavated material, that is defined as the material that is displaced during an impact. This material is not necessarily ejected, so even lower amounts of ejected material can be expected from one bombardment event as suggested by the TLC with a  $2 \times 10^{23}\text{g}$  mass of impactors. However, this already raised the high influence that impacts from a population of small bodies may have on crustal stripping.

Recently, a first step toward constraining the effect of collisional erosion on the Sm/Nd ratio of Earth was achieved, in a realistic dynamical context, using sophisticated erosion scaling laws (fitted to SPH simulations of impacts between similarly-sized bodies) coupled to N-body numerical simulations of Earth's accretion (Carter et al., 2018). However, computational resources limited the resolution (i.e. number of particles forming planetary bodies) in such simulations: collisions in which the impactor was less than 1% of the target mass were neglected (Carter et al., 2018). As a consequence, SPH numerical simulations do not address the physics of smaller cratering impacts (Holsapple and Housen, 2007; Housen and Holsapple, 2011; Svetsov, 2011), thus hampering quantitative estimates of total eroded material. Planetesimals likely contribute to the majority of

impacts, and so collisional erosion may accordingly be driven by small impactors. The effect of these small impacts on the budget of RLE has been neglected in previous works (Carter et al., 2018). In addition, Carter et al. (2018) only explored the collisional stripping of the early Earth proto-crust during the first stages of planetary growth (between 1 Myr and 23 Myr) (Carter et al., 2018) while the presence of numerous planetesimals in the early solar system is predicted up to at least 200 Myr. Only during this period of time and only considering relatively high mass ratio impacts, they already show that a substantial amount of crustal stripping can be reached (6-9% of the planetary mass). That raises the question on the effects that smaller impacts may have in addition to giant impacts.

Here we evaluate the hypothesis that crustal erosion from planetesimal impacts can eventually fractionate Earth’s Sm/Nd ratio. The evolution of the Sm/Nd ratio is monitored during the accretion of Earth (from 1-3 Myr to 200 Myr) using an approach combining analytical modeling of the cratering process and N-body planet formation simulations.

In section 2 we describe the numerical model as well as the two dynamical scenarios explored. In section 3 we present our results for both Grand Tack and classical model. Then we summarize our results and discuss them in the context of the collisional erosion hypothesis and nucleosynthetic anomalies hypothesis.

## 2. Method

### 2.1. Code description

We use N-body numerical simulations from Raymond et al. (2009); Jacobson and Morbidelli (2014) to provide the collisional history of terrestrial embryos (whose sizes are defined for each scenario later on) in the proto-planetary disc. These simulations last for about 200 Myr, and have initial conditions representing the state of the solar disk 3-4 Myr after CAIs. Erosion from small impactors (these do not include the impacts fragments that may contribute to the population of small planetesimals) is tracked through the entire accretion process until proto-Earth embryos reach Earth-like mass. We explore two scenarios for the giant planet’s orbital evolution : (1) the Grand Tack (Jacobson and Morbidelli, 2014) and (2) a classical scenario where the orbits of the giant planets are excited by mutual perturbations (Raymond et al., 2009).

The impacts are divided in two groups : giant embryo-embryo impacts and planetesimal-embryo impacts. The respective ranges of mass for embryos and planetesimals are dependent on the N-body simulation and are described later on. The planetesimal-embryo impacts are treated with an analytical cratering model based on scaling laws for rocky targets (Svetsov, 2011; Holsapple and Housen, 2007). In our model, giant impacts have no effect on the BSE Sm/Nd ratio as they are assumed to fully melt and mix the crusts and mantles of the colliding embryos. This assumption is a simplification that is made because the melting processes resulting from giant impacts are still poorly constrained. Since evidences have been enlightened by previous studies arguing for only incomplete mantle melting even for very energetic impacts (e.g. Nakajima and Stevenson, 2015; Carter et al., 2020), a first step toward estimating the influence of this hypothesis is made by proposing the three distinct sets of assumptions for the chemical mass balances. The results are presented in the supplementary material. After quantifying the mass transfer following each impact, a geochemical model is used to follow the evolution of the amounts of Sm and Nd in the crust and mantle of the different embryos. As numerous works suggest an early differentiation of

planetary bodies (Lugmair and Shukolyukov, 1998; Srinivasan et al., 1999; Bizzarro et al., 2005; Amelin, 2008; Kruijer et al., 2014), we assume that all embryos in the simulations are differentiated. The processes of crust-mantle reequilibration after an impact are poorly known. Consequently, we assume that giant impacts induce a full crust-mantle reequilibration, while planetesimals impacts only affect the composition and mass of the crust and leave the mantle unchanged. Since the N-body numerical simulations used here assume perfect merging, there is no way of tracking the ejected material. In consequence possible capture of ejected material by other embryos, following an impact, has been neglected. Accordingly, the fractionation computed in this work might be overestimated. We introduce  $\epsilon$  the parameter describing the chemical fractionation of the Sm/Nd ratio in the mantle of growing Earth like embryos (i.e. BSP for Bulk Silicate Planet) with respect to the initial chondritic composition:

$$\epsilon = \frac{\left(\frac{Sm}{Nd}\right)_{BSP}^t - \left(\frac{Sm}{Nd}\right)_{BSP}^{ini}}{\left(\frac{Sm}{Nd}\right)_{BSP}^{ini}},$$

with  $\left(\frac{Sm}{Nd}\right)_{BSP}^t$  the Sm/Nd ratio of the BSP at any time  $t$  of the simulation and  $\left(\frac{Sm}{Nd}\right)_{BSP}^{ini}$  the Sm/Nd ratio of the BSP at time zero of the simulation (i.e. chondritic value).

The details of the model (i.e. quantification of ejected and accreted masses, chemical mass balances and post-processing N-body simulations of accretion) are presented hereafter.

## 2.2. Cratering model

The first step of the work consists in the calculation of the eroded and accreted masses during a single impact event. As we consider embryos as differentiated bodies, the eroded mass is assumed to have a crustal composition when the total ejected mass after considering all impacts from a given distribution is lower than the crustal mass. This assumption is made to take into account the fact that overlapping between the craters may occur since it physically implies that the model assumes that all planetesimals from a given distribution are coming from all direction. For greater ejected masses, the eroded material is assumed to be made of both crust and mantle (the remnant mass after the entire crust is considered is then ejected mantle). We assume that planetesimals have a bulk chondritic composition which imply that accreted mass has a chondritic composition. The ejected and accreted masses are deduced from previous studies analytical laws constructed as a function of the impact velocity at encounter, the impactor density and the target density and masses of both the target and impactor (Holsapple and Housen, 2007; Shuvalov, 2009; Svetsov, 2011).

These parameterizations assume that the impactor mass is much smaller than the target mass (i.e.  $M_i/M_e < 0.01$ ) so they cannot be used for giant impacts. The treatment of the giant impacts in the proposed model is dependant on the mixing scenario choosen. This point is described in the section 2.3.

## 2.3. Mass balance model

O'Neill and Palme (2008) proposed a mass balance for a two-stage model of crustal erosion: with (1) crust-forming process and (2) collisional erosion. The first stage assumes the formation of the embryo's crust with fractionation between compatible and incompatible elements. The newly formed proto-crust is enriched in incompatible elements relatively to the residual mantle. In the

calculation proposed by O'Neill and Palme (2008),  $f_{p-c}^1$  represents the fraction of proto-crust with respect to the entire embryo's mass. We adapt this melting equation to our specific problem and define the term  $f_{p-c}^1$  as the melt fraction normalized to the primitive mantle mass only, except for the first stage (before any impact) made to estimate the initial composition of the embryo's crust. In the second stage, a  $f_{p-c}^2$  fraction of the proto-crust is eroded (note that  $f_{p-c}^2 < f_{p-c}^1$ ). The concentrations of an element  $M$  in the crust and mantle after the first stage can be described following:

$$\frac{C_M^{p-c}}{C_M^0} = \frac{1}{D_M + f_{p-c}^1(1 - D_M)}, \quad (1)$$

With  $D_M$  the partition coefficient of  $M$  between melt and solid,  $C_M^0$  the chondritic composition for  $M$ , and  $C_M^{p-c}$  its concentration in the proto-crust. It is possible to estimate the concentration in the BSP (Bulk Silicate Planet, i.e. crust and mantle of the growing planetary embryo) after the second stage as (assuming no mantle erosion):

$$\frac{C_M^{BSP-eroded}}{C_M^0} = \frac{f_{p-c}^1(1 - D_M) + D_M - f_{p-c}^2}{(D_M + f_{p-c}^1(1 - D_M))(1 - f_{p-c}^2)}, \quad (2)$$

Where  $C_M^{BSP-eroded}$  is the concentration of  $M$  in the BSP.  $f_{p-c}^1$  is initially fixed to a value of 0.026 following O'Neill and Palme (2008). It is then assumed that the partial melting rate remains constant over the accretion history (inducing variations in the crust thickness because of the embryo mass increase) but  $f_{p-c}^1$  takes a value of 0.037. Three different scenarios are considered for crustal formation after an impact, with notably two of them being end-members (we call them scenario 1 & 2. ).

Further results (section 3) are presented for the most realistic case only (called scenario 3), however they are all discussed in appendices.

### 2.3.1. Scenario 3: "remixing only for giant impacts" model

This scenario is an intermediate case in between (1) and (2) that respectively refer to two extreme end members. For the scenario 1, all impacts are assumed to melt the entire proto-Earth mantle and to fully re-equilibrate the chemical composition in the BSP. Scenario 2 assumes that none of the impacts produce any mantle remixing. Accordingly, we propose an intermediate case that is much more realistic: scenario (3). Planetesimal-embryo impacts are treated following scenario (2), see eq. 12 while Embryo-Embryo impacts are treated following scenario (1)(i.e. full melting of the BSP with formation of a new crust). Accordingly, the composition of the mantle changes each time a giant impact occurs. All giant impacts are considered as perfect mergers. For simplifications, we assume that this results in a mass of chondritic composition equal to the impactor mass is accreted to the target.

### 2.4. Planetesimals size-frequency distribution

N-body simulations need high computational requirements, so they can not include a realistic amount of planetesimals for the calculations. This is why we have chosen here to distribute the mass of a single planetesimal impactor into a size-frequency distribution of smaller impactors (i.e. each impact from a planetesimal in the data file is assumed to be a serie of impacts with impactors distributed on a size-frequency distribution (SFD)). That serie of impactors is assumed to fall

onto the target at the same time. Considering the mass transfer, this assumption implies that the erosion caused by all impactors in the SFD of a given superparticle is applied first. Then accreted mass is added.

The differential size distribution of impactors follows a power law :

$$\frac{dN_{sfd}( > r )}{dr} = -Kr^{-\alpha}, \quad (3)$$

with  $\alpha$  and  $K$  standing for positive constants.  $N_{sfd}( > r )$  is the cumulative size distribution (the number of bodies with a radius larger than  $r$ ). We get upon integration :

$$N_{sfd}( > r ) = K \left( \frac{r_{max}^{1-\alpha} - r^{1-\alpha}}{1-\alpha} \right) \quad (4)$$

and the total mass of the distribution can be described as

$$M_T = \int_{r_{min}}^{r_{max}} -\frac{4}{3}\pi r^3 \rho \frac{dN_{sfd}}{dr} dr, \quad (5)$$

with  $\rho$  standing for the mean density of the planetesimals. So replacing  $\frac{dN_{sfd}}{dr}$  in the later expression we get,

$$M_T = \int_{r_{min}}^{r_{max}} \frac{4}{3}\pi r^3 \rho K r^{-\alpha} dr. \quad (6)$$

It is then possible to obtain  $K$ :

$$K = \frac{3M_T}{4\pi\rho} \times \frac{4-\alpha}{r_{max}^{4-\alpha} - r_{min}^{4-\alpha}}, \quad (7)$$

where  $M_T$  (the total mass of the distribution) equals the mass of the impactor given in the N-body simulation.  $r_{min}$  and  $r_{max}$  have to be fixed. They are arbitrarily chosen as 8m and 800km respectively. The number of bodies in each mass bin is evaluated using the cumulative mass distribution, rounded to an integer number using a random number generator. Accordingly, 800km is taken as the upper bound of this distribution to be slightly lower than the typical size of a planetesimal in the simulations (Raymond et al., 2009; Jacobson and Morbidelli, 2014). It may be noted that a 800km-sized body is likely differentiated. However, whether the planetesimals are differentiated or not makes no difference in our model since we only investigate here the evolution of an elemental ratio of two RLEs. However the change in the minimum radius of a body within the SFD is not critical on the model outcomes (less than 1% change in the fractionation when choosing minimum radius values of few kilometers). The physical characteristics of the planetesimals are as follows :

- The mean density of the target,  $\rho_m$ , is assumed to be 5200 kg/m<sup>3</sup>.
- The crust density,  $\rho_t$ , is assumed to be 2900 kg/m<sup>3</sup>.
- The density of impactors (chondritic material),  $\rho_{imp}$ , is assumed to be 2600 kg/m<sup>3</sup>.
- The impact velocity is assumed to be:  $V_{imp} = \sqrt{V_{inf}^2 + v_{esc}^2}$  with  $V_{inf}$  the velocity of the impactor at infinity (beyond the gravitational attraction of embryos), which is here assumed to be the same for all impactors in the same impact event. This  $V_{inf}$  is deduced from the data of the N-body simulation.

- The radii of target and impactors are calculated using their mean densities and respective masses.

In this study, the slope of the SFD ( $\alpha$ ) is set at 3.5 which corresponds to the actual value of the distribution of bodies in the asteroid belt. However, the influence of the choice for  $\alpha$  needs to be examined, this is the subject of the section 4.2 in the appendices.

## 2.5. Dynamical Scenarios

The impact model presented in the previous section is applied to two dynamical accretion scenarios of the terrestrial planets accretion: (1) Grand Tack or (2) classical. Within each dynamical model, a variety of parameters are explored such as (i) variable eccentricities and semi-major axis of Jupiter and Saturn (for classical model), (ii) different surface densities of the disc (classical) and (iii) different initial embryo masses (Grand Tack). These different dynamical scenarios are summarized in Table 1 (Classical) and Table 2 (Grand Tack) with their associated results for our model in terms of fractionation in Sm and Nd.

The classical model (e.g. Wetherill, 1978, 1985, 1996; Kokubo and Ida, 2000; Chambers and Wetherill, 2001; Raymond et al., 2009) is the reference model concerning terrestrial planets formation, however it is well known now that it fails in reproducing several key features of our present day solar system. Other models have been further proposed to better reproduce the structure of the Solar System at its present state. Notably, the Grand Tack model is very popular as it among the first models proposed that can explain the small masses of Mars and the asteroid belt. It also reproduces the excited orbits of the bodies in the main asteroid belt, as well as the mixing between inner and outer solar system objects.

### 2.5.1. Classical scenario

The main assumption considered in the Classical model is that the formation of the terrestrial planets can be treated independently compared to the giant gaseous planets (Wetherill, 1990, 1992; Chambers and Wetherill, 2001; Raymond et al., 2006, 2009, 2014). The initial conditions thus assume that Jupiter and Saturn are already formed and placed on fixed orbits. Then, it assumes that the terrestrial planets formed essentially from material originated close from their current position within the disk. Such a growth dynamics induces similar sizes for bodies on adjacent orbits (Kokubo and Ida, 2002). Classical models fail to reproduce the size of Mars.

In our study all simulations start with a disk (from 0.5AU to 4.5AU) of embryos and planetesimals with Jupiter and Saturn already formed. They contain 85-90 embryos and 1000-2000 planetesimals (Raymond et al., 2009). The total mass of the system is equally distributed between planetesimals and embryos. However, eight different sets of initial conditions are explored (Raymond et al., 2009). They refer to different orbits of Jupiter and Saturn and different disk surface densities (See Table 1 for details). Depending on the initial conditions, the initial mass of the embryos in the disk is comprised between 0.005 and 0.1 terrestrial masses.

### 2.5.2. Grand Tack scenario

The grand tack scenario was designed to explain the small size of Mars as this was one of the major issues with the classical accretion model (Walsh et al., 2011; Raymond and Morbidelli, 2014). The inward migration of Jupiter, followed by Saturn before they both migrate outward - when Jupiter gets caught in the 2:3 resonance with Saturn (Masset and Snellgrove, 2001; Morbidelli and Crida, 2007; Pierens and Raymond, 2011)- has been proposed as a mechanism to deplete and excite



the Mars region leading to a small size of Mars and a distribution of orbital elements in the asteroid belt compatible with current observations. In the simulations we use here, the system contains a population of embryos and two different populations of planetesimals (i.e. internal planetesimals - within 3 AU - and external smaller planetesimals beyond 3 AU) (Jacobson and Morbidelli, 2014). Each simulation begins with approximately 100 embryos and 2000 planetesimals. The N-body numerical simulations data used here consider the system is equally distributed between the different planetesimals and embryos masses (Jacobson and Morbidelli, 2014). However, the initial typical mass of an embryo before the onset of Jupiter’s inward migration is a free parameter. Three different values are tested here:  $0.025M_{\oplus}$ ,  $0.05M_{\oplus}$  or  $0.08M_{\oplus}$  (referenced respectively as 0.025, 0.05 and 0.08 in Table 2). The corresponding average  $\epsilon$  values and their  $1\sigma$  uncertainty are detailed in Table 2.

### 3. Results and discussion

Fig. 1 shows how  $\epsilon$  evolves during the accretion of eight representative planets extracted from different N-body simulations: (i) four embryos evolved within a Grand Tack scenario with different initial masses and (ii) four other embryos evolved within a classical scenario for different Jupiter and Saturn orbits. Only a small fraction of the impacts have a significant influence on the fractionation. This effect is a consequence of the impact configuration, especially the impact velocity: the higher the velocity, the more crust is typically ejected. However, successive impacts by planetesimals produce a fractionation that cannot be neglected. The less massive the embryo the easier it is for impactors to erode the surface, leading to a higher fractionation in Sm and Nd in the BSP. The impact history varies considerably from planet to planet and from simulation to simulation. In the case of the Grand Tack scenario, most of the fractionation is produced during the first Myrs, when the system is dynamically excited by the migration of the giant planets. In the classical scenario, the fractionation occurs over the entire accretion history and the final BSP concentration becomes stable later than for the Grand Tack scenario.

On average neither the classical accretion model ( $\epsilon = 0.029 \pm 0.015$ ) nor the Grand Tack ( $\epsilon = 0.024 \pm 0.013$ ) can account for the eventual superchondritic BSE Sm/Nd ratio ( $\epsilon = 0.06$ ), especially not within the first 30 Myrs of accretion. The final  $\epsilon$  values are presented in the fig. 2 as a function of the final masses of embryos at the end of the 71 N-body numerical simulations. Most of the surviving embryo’s masses range between  $0.03M_{\oplus}$  and  $1.4M_{\oplus}$ . Smaller final embryos present a much larger range of  $\epsilon$  values, especially in the case of the Grand Tack scenario (fig. 2). This is due to the fact that collisional erosion and consequent chemical fractionation is more efficient for smaller embryos. For the Grand Tack scenario especially, the system is very excited during the first Myrs because of the early migration of Saturn and Jupiter. At this time, the embryos can easily be eroded because of their lower masses and escape velocities. However, for bodies considered as relevant Earth analogs (i.e. with a final mass between  $1/2M_{\oplus}$  and  $1.2 \times M_{\oplus}$  and final semi-major axis between 0.5 AU and 2 AU), the range of variation of  $\epsilon$  values is narrower than for smaller bodies and  $\epsilon$  almost never reaches the Earth target value of 0.06.

Note however that we have used a partial melting rate of 2.6% as proposed by O’Neill and Palme (2008) to produce the newly formed crust. Such a low partial melting rate is maybe appropriate for the Earth (O’Neill and Palme, 2008) whereas it differs significantly from estimates of differentiated bodies such as Vesta (possibly up to 20%), Ceres or the Moon (between 5% to 10%) (Yamaguchi et al., 1997; Ruzicka et al., 1997). However, increasing the partial melting rate in our model

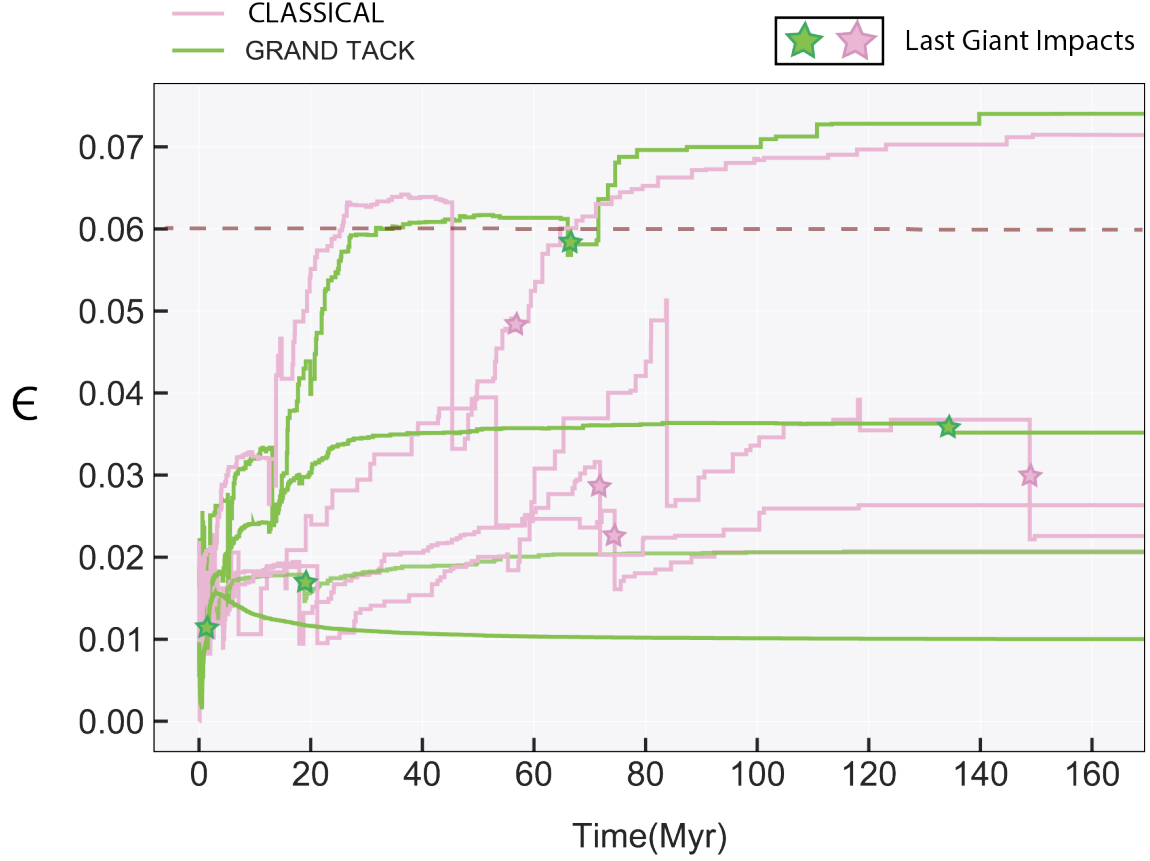


Figure 1: Evolution of the fractionation parameter  $\epsilon$  as a function of time for 8 relevant Earth analogs accretion histories: four evolving within a classical accretion scenario with different orbits of Jupiter and Saturn and four evolving within a Grand Tack scenario. They respectively end up with masses of  $0.6M_{\oplus}$ ,  $0.69M_{\oplus}$ ,  $1M_{\oplus}$ ,  $1.01M_{\oplus}$ ,  $1.2M_{\oplus}$ ,  $1.2M_{\oplus}$ ,  $1.01M_{\oplus}$ ,  $0.86M_{\oplus}$  and semi major axis of 1.16 AU, 0.6 AU, 0.76 AU, 0.62 AU, 0.72 AU, 0.9 AU, 0.95 AU and 0.71 AU, from the most fractionated to the less fractionated. A zero fractionation value refers to a chondritic composition. Time zero is the beginning of the simulation:  $\simeq 3$  Myr after CAIs. In the case of the Grand Tack scenario, time zero corresponds to the very beginning of the Jupiter's migration. Stars refer to the last giant impact for Grand Tack and classical scenarios.

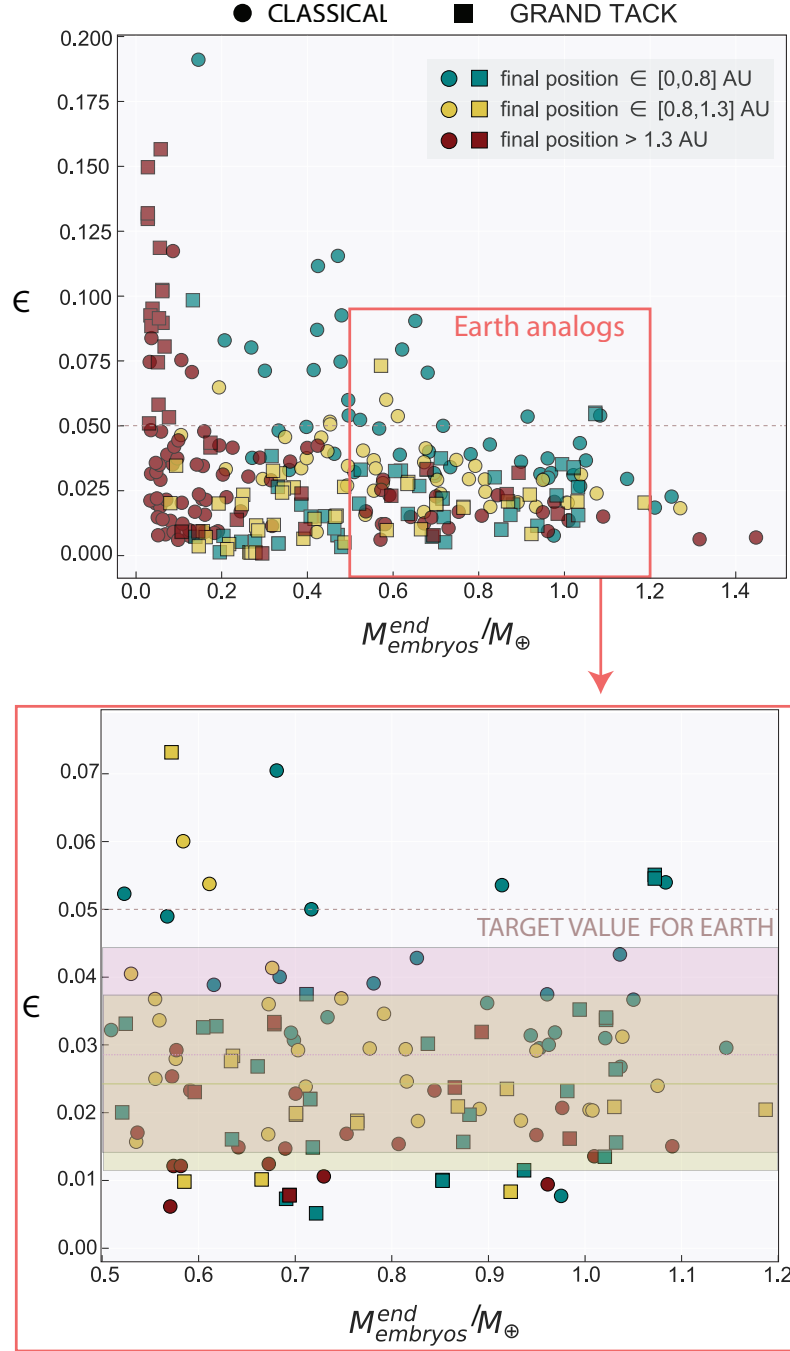


Figure 2: Top panel: Sm-Nd fractionation with respect to chondritic Sm/Nd values of the different embryos surviving at the end of 40 classical and 31 Grand Tack N-body simulations reported as a function of their final masses. The markers refer to the type of accretionary scenario (circles for the classical scenario and square for grand tack). The colors refer to the final semi-major axis of the embryos. The bottom panel is a zoom of the top panel corresponding to the good Earth analogs. The green line is the average value of  $\epsilon$  for the grand tack simulations, the associated light green area is the  $1\sigma$  uncertainty. The pink line and light pink area refer respectively to the average and  $1\sigma$  uncertainty for the classical accretionary scenario.

would lead only to a decrease in the fractionation of the Sm/Nd ratio (i.e.; lower epsilon value) and could accordingly never account for the observed Sm/Nd value of the BSE. Thus, collisional erosion seems unlikely to explain the possible superchondritic Sm/Nd ratio of the BSE except in marginal cases discussed hereafter. Moreover, the present model assumes strictly chondritic composition for the accreted material which may be invalid especially in the case of embryo-embryo impacts. A higher fractionation could be expected without this assumption because the impacting embryo might have been fractionated in their own earlier accretion history. Considering the present results, estimating the accurate influence of this parameter cannot be done. This will be the object of further investigation in future works. Additionally, O'Neill and Palme (2008) predicted a need of 54% of the crust mass to be ejected in order to account for a 6% fractionation into the Sm/Nd ratio. This corresponds to about 1.5% of the Earth's mass that should be ejected as crustal material. This is way lower than our estimates of ejected masses that can go up to 17% in most erosive cases, even if the fractionation in Sm/Nd predictions remain under the 6%. For Grand Tack simulations, and if we consider only Earth analogs, the average fraction of ejected mass relative to the final mass of the embryo is  $7.5\% \pm 6.9\%$ . It should be noted here that O'Neill and Palme (2008) assume a single impact on a potential Earth analog that would have its current mass. It implies that the effect of accreted material through time (possibly reducing the enrichment of the crust and BSE in Nd relative to Sm during accretion) is fully neglected. Additionally, melting and re-equilibration processes during accretion are not mentioned in this model neither (O'Neill and Palme, 2008). These different results cannot be directly compared to each other.

Using our results, we also evaluate the hypothesis of enstatite chondrites as the dominant accreting material for Earth as they share strictly similar isotopic compositions with Earth (Javoy, 1995; Javoy et al., 2010). In this case, collisional erosion has been proposed to account for the elevated Mg/Si ratio of the BSE compared to enstatite chondrites (Boujibar et al., 2015) if 15% of the early Earth mass is eroded (Boujibar et al., 2015). Only 9% of the total planetary mass was predicted to be eroded from recent numerical simulations (Carter et al., 2018) neglecting the impacts of small planetesimals. Our results show that an erosion of 17% of the final embryo's mass can be reached. Furthermore, this 15% estimation (Boujibar et al., 2015) is based on considering a single impact stripping away that amount of a crust already highly enriched in Si compared to Mg (because of the large difference in the degree of compatibility of Si and Mg at the high pressure and temperature conditions considered for differentiation (Boujibar et al., 2015)). Additionally, the accretion onto its surface of chondritic material is not considered by Boujibar et al. (2015) and should lead to a lower fractionation (as illustrated in the present work with the Sm/Nd ratio). Thus, preferential erosion of the crust induced by low energy impacts is unlikely to fully account for the observed Mg/Si ratio of the BSE if Earth was mainly accreted from enstatite chondrites. However, an alternative scenario has been proposed by Dauphas et al. (2015) that may explain the Earth Mg/Si non chondritic ratio by nebular fractionation effects, requiring in that case no or low collisional erosion to happen during accretion.

For Grand Tack simulations (but not classical model simulations), we find a positive correlation between the chemical fractionation in Sm and Nd of the BSP and the timing of the last giant impact (fig. 3). However there is no correlation between the number of giant impacts and the final fractionation. Thus, the observed correlation between the timing of the Moon-forming event and the fractionation is the consequence of the fact that late last giant impacts are due to a lack of dynamical friction in the disk (Jacobson and Morbidelli, 2014), which consequently creates more erosive collisions. An other key factor for this correlation to the timing of the last giant impact

is the crustal growing rate as it grows mostly through the input of chondritic material. Indeed, such amount of chondritic material input further leads to a decrease of the incompatible elements concentration within the crust. This means that for every giant impact a newly more incompatible-rich crust is formed. This makes easier the chemical fractionation for the next impacts responsible for a preferential loss of crust relative to the mantle. Considering chemical measurements on terrestrial and lunar samples (for Hf/W, Mg-suite crustal rocks, highly siderophile elements, I-Xe) (Chyba, 1991; Walker, 2009; Touboul et al., 2007, 2009, 2012, 2015; Pepin and Porcelli, 2006), lunar rocks dating (Norman et al., 2003; Nyquist et al., 2006; Borg et al., 2011; Boyet et al., 2015; Carlson et al., 2014) and numerical simulations (Jacobson et al., 2014; Jacobson and Morbidelli, 2014), estimates of the age of the moon support a late forming giant impact ranging in between 50 Myr and 150 Myr (after the CAIs formation), with a preferred value around 100 Myr (Carlson et al., 2014; Touboul et al., 2012; Pepin and Porcelli, 2006; Jacobson and Morbidelli, 2014). In addition, two recent studies have argued for a younger estimate of the Moon time formation that would be 50 Myr after CAIs (Barboni et al., 2017; Thiemens et al., 2019). These are based on methods (from Lu-Hf system or Hf-W) that have the advantage of presenting relatively low uncertainties. In addition, U-Pb estimates for the age of the terrestrial silicate differentiation is  $4480 \pm 20$  Myr (e.g. Manhès et al., 1979; Albarede and Martine, 1984; Allègre et al., 2008), suggesting that the Moon-forming impact is unlikely to have occurred after 80 Myrs. The age of the Moon is still debated, however most estimates point out to a no younger than 50 Myr Moon-formation. In our Grand Tack simulations the superchondritic Sm/Nd ratio of the BSE can be produced only in the case of a last giant impact occurring after 60 Myrs in agreement with most of these recent estimates. While only a modest fraction (2%) of our sample of Grand Tack simulations have Earth analogs that suffer a last giant impact after 100 Myr, those accretion histories are favored for another reason. Planetesimals that collide with Earth after the last giant impact deliver highly-siderophile elements (HSEs) to Earth's crust and mantle; matching the very low abundance of HSEs in the BSE (Walker, 2009) requires a late last giant impact (Jacobson et al., 2014). However, after 103 Myr half of the  $^{146}\text{Sm}$  should have decayed into  $^{142}\text{Nd}$  already. This implies that further fractionation between elemental Sm and Nd should have no (or low) effect on the  $^{142}\text{Nd}/^{144}\text{Nd}$ . In that case, Sm/Nd ratio evolution cannot be a proxy for the  $^{142}\text{Nd}/^{144}\text{Nd}$  after a few tens of Myr and should only be interpreted as an elemental fractionation. Additionally, if an excess in Sm/Nd ratio is produced after 30 Myr, it would cause an anomaly in  $^{143}\text{Nd}/^{144}\text{Nd}$  larger than observed (Boyet and Carlson, 2005). The addition of the evidences for nucleosynthetic anomalies as responsables for the excess in  $^{142}\text{Nd}/^{144}\text{Nd}$  and the observables on  $^{143}\text{Nd}/^{144}\text{Nd}$  ratio lead us to favor a low erosive process during terrestrial planets accretion (i.e. no late last giant impact). However, it is important to mention here the fact that no erosion is assumed in our model during giant embryo-embryo collisions. This has been done by Carter et al. (2018) for the 20 first Myr of evolution of the proto-planetary disk. They find fairly similar results than we do, implying that if the results of both studies are applicable together, then the combined effect of larger impacts and cratering impacts could be sufficient to explain a high Sm/Nd ratio acquired during the 30 first Myr. This adds an other argument to the fact that a low erosive environment should be favored for the accretion process not to produce higher anomalies than any observed. Additionally, as mentioned before, the partial melting rate assumed in our present model is low. A simple way to decrease the fractionation in Sm and Nd even for highly erosive cases could be to significantly increase (by several percents at least) the partial melting rate when forming new crusts. The effects of the partial melting rate are presented in the supplementary materials.

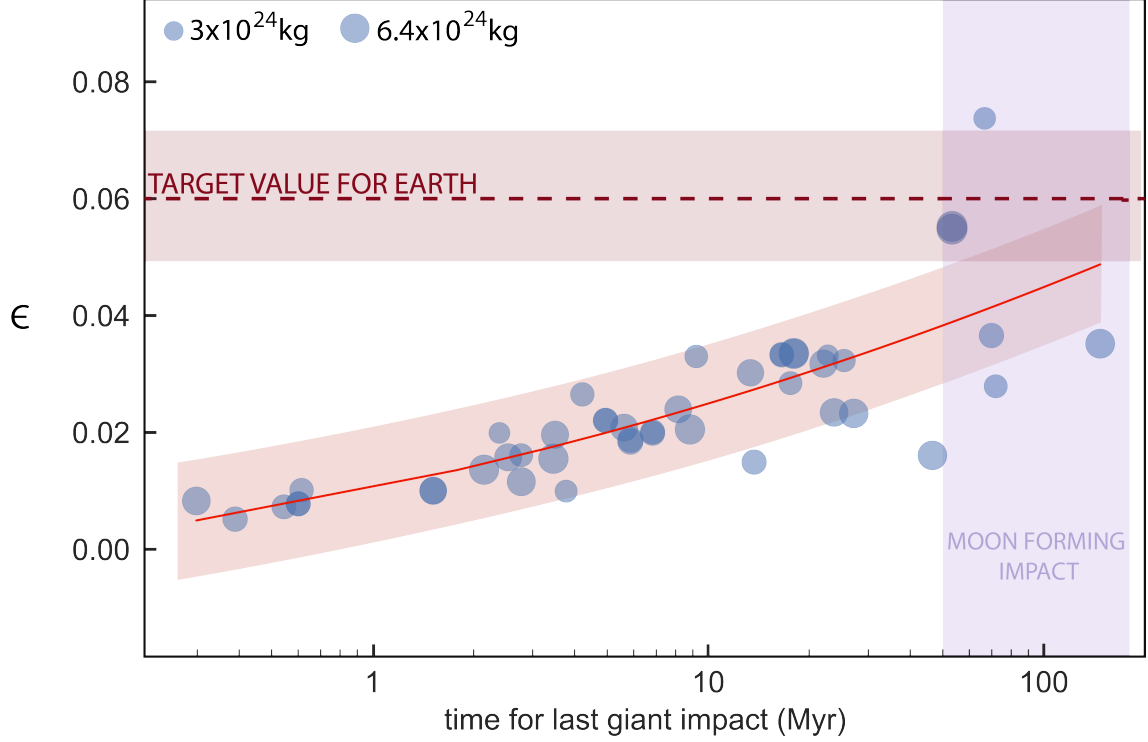


Figure 3: Sm-Nd fractionation with respect to chondritic Sm/Nd values of the different Earth analogs at the end of Grand Tack N-body simulations reported as a function of the timing of the last giant impact suffered. The markers sizes refer to the final mass of an embryo. The purple area refers to the time laps of the moon forming impact. The red curve is our quadratic fit for the relation between the fractionation value and the timing of the last giant impact, the light red envelop defines the  $1\sigma$  error associated.

Nucleosynthetic anomalies has been emphasized as an explanation for the excess in  $^{142}\text{Nd}$  of the Earth (Burkhardt et al., 2016; Bouvier and Boyet, 2016). That case would require at most 2% of chemical fractionation of the Sm/Nd ratio induced by collisional erosion in order to maintain the initially implanted Sm/Nd ratio in planetary bodies by nucleosynthetic anomalies (Burkhardt et al., 2016; Bouvier and Boyet, 2016). Therefore, the dynamical and geochemical scenarios leading to such a low final fractionation need to be explored and might provide another set of constraints on the initial conditions of the solar system.

Impacts with a high velocity (higher than 20 km/s at encounter) are highly erosive (Svetsov, 2011; Shuvalov, 2009). However, they represent only a small fraction of the total. Overall, the impact velocity averaged over 200 Myrs and over the whole disk is higher for non Grand Tack scenarios and for a steeper disc surface densities. Additionally, since the embryos grow faster in the frame of the Grand Tack than in the classical scenario, is it made earlier harder to eject material. As a consequence of these two aspects, the Grand Tack scenarios generally induce a slightly lower fractionation among the different embryos, but the timing of the onset of the Grand Tack might also influence the fractionation yields. Erosion may be more efficient when the system is excited early as embryos have smaller sizes than in a later case. Therefore, future works could constrain the timing of the onset of the Grand Tack (if it existed) in order to preserve the original Sm/Nd fractionation implanted by nucleosynthetic anomalies or, in opposition, to induce efficient stripping of the crust.

Modeling the effects of collisional erosion for other RLE will eventually provide further insights on whether a given terrestrial accretion history can be compatible with observed nucleosynthetic

anomalies in chondritic components.

### 3.1. Outcomes dependency on the dynamical scenario

We emphasized that in the case of the remixing scenario reliable on, the grand tack tends to produce a slightly lower final fractionation for relevant Earth analogs compared to the classical scenario (see tables 1 & 2). However, in the case of smaller embryos, the range of final  $\epsilon$  values is larger in the grand tack dynamical scenario than in the classical dynamical scenario. Collisional erosion and consequent chemical fractionation is more efficient for smaller embryos. Within a Grand Tack dynamical scenario, the embryos reach a Earth-like mass faster (within 20-25Myr) and become accretive faster, limiting sooner the erosive power of collisions. The erosive power of collisions is improved at earlier times in the grand tack dynamical scenario since the system is excited by the migration of the giant planets Jupiter and Saturn. This combined effect is responsible for the differences between the dispersion observed in fig 2 for Classical Grand Tack scenarios. However, besides the higher dispersion for the Grand Tack scenario, the final average fractionation is lower for the Grand Tack than for the classical scenario. This is a surprising result that can be explained by the fact that in the Grand Tack scenario the embryos grow much faster. After 20 Myr the embryos ending as good Earth analogs have already reached most of their total masses. From that point, it becomes complicated to produce enough erosion to induce significant fractionation (because of (1) the composition of the crust that is most of the time close to chondritic because of accretion and of (2) the escape velocity that tends to limitate the erosive power of a given impact).

## 4. Conclusion

We have quantified the efficiency of collisional erosion during Earth accretion for two dynamical scenarios ( classical scenario and Grand Tack scenario) and computed the resulting BSE Sm/Nd ratio using a combination of analytical modeling of cratering processes (Housen and Holsapple, 2011; Svetsov, 2011), simple mass balance estimates (O'Neill and Palme, 2008) and N-body numerical simulations (Raymond et al., 2009; Jacobson and Morbidelli, 2014). It is shown (Fig. 1) that only a small amount of impacts (compared to the total) is responsible for a significant fractionation of the BSP Sm/Nd ratio, notably for the classical scenario. During the Grand Tack scenario, most of the fractionation is acquired during the first Myrs (owing to the low escape velocities of small embryos and the rapid decrease of the planetesimal population) of the system evolution while the classical scenario presents a more progressive fractionation trend, spreading all over the accretion history. We find, that a maximum of 17% of the proto-planet's mass erosion can be reached for the most erosive cases. In average, over all surviving embryos, only 5% of the proto-planet's mass is ejected as crust. Even though this amount of ejected crust is large, we show that neither the classical model, nor the Grand Tack model can always account, for the  $^{142}\text{Nd}$  possible excess in terrestrial rocks. However, we find a strong correlation between the fractionation in Sm and Nd with the timing of the Moon-forming event in the case of the Grand Tack scenario. Especially, a large  $\epsilon$  fractionation (about 5%) is reachable for a Moon-forming impact (last-giant impact) occurring after 50 Myr after CAIs, that could account for the proposed off-set in  $^{142}\text{Nd}$ . New evidences of nucleosynthetic heterogeneities in primitive planetary components obviates the need for a superchondritic Sm/Nd ratio of the BSE and impose limited loss of crust preferential erosion during accretion. Such observations seem to challenge the most eroding scenario explored in this

		cjs1	cjs15	cjsecc15	jsres	jsresec	eejs15	ejs1	ejs15
(1)	$\bar{\epsilon}$ mean fraction-ation	0.029	0.04	0.04	0.041	0.05	0.05	0.04	0.05
	Standard deviation	0.003	0.01	0.01	0.009	0.02	0.015	0.016	0.02
(2)	$\bar{\epsilon}$ mean fraction-ation	0.007	0.0049	0.004	0.0037	0.004	0.005	0.009	0.009
	Standard deviation	0.002	0.0008	0.001	0.0003	0.0015	0.002	0.006	0.006
(3)	$\bar{\epsilon}$ mean fraction-ation	0.020	0.025	0.021	0.025	0.030	0.028	0.03	0.03
	Standard deviation	0.002	0.004	0.006	0.005	0.008	0.008	0.01	0.01
Grand tack ?		no	no	no	no	no	no	no	no
Description		Circular Jupiter and Saturn. Mutual inclination = $0.5^\circ$ . $a_j=5.45$ AU and $a_s=8.18$ AU. $\chi = 1$	Same as cjs1 but with $\chi = 3/2$ (MMSN model)	cjs with eccentric orbits. Jupiter and Saturn placed at their semimajor axis 5.45 AU and 8.18 AU with $e_j=0.02$ and $e_s=0.03$ and a mutual inclination of $0.5^\circ$	Jupiter and Saturn in resonance, placed in their mutual 3:2 mean motion resonance. $a_j=5.43$ AU, $a_s=7.30$ AU and $e_j=0.005$ , $e_s=0.01$ with a mutual inclination of $0.2^\circ$	Jupiter and Saturn in resonance on eccentric orbits. Same as jsres but with $e_s = 0.03$	Extra eccentric Jupiter and Saturn. Placed at their actual semi major axis but with high eccentricity orbits. $a_j=5.25$ AU, $a_s=9.54$ AU, $e_j=0.1$ and $e_s=0.1$ . mutual inclination is $1.5^\circ$	Eccentric Jupiter and Saturn. Initial orbits around actuals. Same semi major axis and mutual inclination than in eejs15. $e_j=0.05$ , $e_s=0.06$	Same as cjs1 but with $\chi = 3/2$ instead of 1.

Table 1: Table of the  $\epsilon$  mean values in the BSP after the growth of the embryos considered as Earth analogs (with a final mass comprised between  $1/2M_\oplus$  and  $1.2M_\oplus$  and a semi major axis comprised between 0.5 AU and 2 AU) in a classical accretion scenario. The standard deviation associated to each value is also available in the table. (1) refers to the mixing scenario 1, for which a full reequilibration between crust and mantle is assumed after an impact. (2) denotes the opposite scenario for which there is no reequilibration at all, the giant impact are thus ignored and for the small impacts, it is assumed that everything happens in the crust, remaining the mantle intact. Finally, (3) refers to the intermediate scenario. Giant impacts are treated in agreement with scenario (1) and small impacts are treated the same way than in scenario (2). The values are given for each kind of simulations, with different initial conditions. A quick description of each type of N-body simulation is given.  $a_j$  and  $a_s$  refer respectively to the Jupiter and Saturn semi-major axis.  $e_j$  and  $e_s$  denote the eccentricities of Jupiter and Saturn respectively.  $\chi$  is used to varie the effect of the disc surface density. The disc surface density can be expressed as:  $\Sigma(r) = \Sigma_1 \left(\frac{r}{1\text{AU}}\right)^{-\chi}$ . The  $r^{-1}$  simulations formed slightly fewer planets, contained less total mass in planets and had longer formation timescales for Earth for the final systems than the  $r^{-3/2}$  simulations Raymond et al. (2009). "MMSN" refers to the "Minimum Mass Solar Nebula" model Weidenschilling (1977).

work corresponding to a Grand Tack combined with a late moon forming impact. However, it is important to keep in mind the assumptions of the model presented here. Notably, a low fractionation could be achieved even in an erosive dynamical scenario if the partial melting rate for forming the crust is much larger or under alternative crust compositions as suggested by Carter et al. (2018). Further works should investigate systematically the effect of collisional erosion on the budget of other refractory and lithophile elements and provide an acceptable set of conditions for the dynamical accretion of the Earth that could account for the observed compositions of these elements in the BSE.

## Acknowledgement

J.S. acknowledges support from the French National Research Agency (ANR project VolTerre, grant no. ANR- 14-CE33-0017-01) And Institut Universitaire de France. Parts of this work were supported by the UnivEarthS Labex programme at Sorbonne Paris Cité (ANR-10-LABX-0023 and ANR-11- IDEX-0005-02).



		0.025	0.05	0.08
(1)	$\bar{\epsilon}$ mean fractionation	0.11	0.11	0.13
	Standard deviation	0.04	0.02	0.03
(2)	$\bar{\epsilon}$ mean fractionation	0.0019	0.0021	0.0007
	Standard deviation	0.0007	0.0005	0.0002
(3)	$\bar{\epsilon}$ mean fractionation	0.03	0.021	0.013
	Standard deviation	0.01	0.007	0.008
Grand tack ?		yes	yes	yes
Description		initial em- bryos masses = $0.025M_{\oplus}$ .	initial em- bryos masses = $0.05M_{\oplus}$	initial em- bryos masses = $0.08M_{\oplus}$

Table 2: Table of the  $\epsilon$  mean values in the BSP after the growth of the embryos considered as good Earth analogs in a grand tack accretion scenario (Jacobson and Morbidelli, 2014). The standard deviation associated to each value is also available in the table. (1) refers to the mixing scenario 1, for which a full reequilibration between crust and mantle is assumed after an impact. (2) denotes the opposite scenario for which there is no reequilibration at all, the giant impact are thus ignored and for the small impacts, it is assumed that everything happens in the crust, remaining the mantle intact. Finally, (3) refers to the intermediate scenario. Giant impacts are treated in agreement with scenario (1) and small impacts are treated the same way than in scenario (2). The values are given for the three different sets of initial conditions concerning the initial mass of an embryo (corresponding to the mass that basically has an embryo when the inward migration of Jupiter begins).  $M_{\oplus}$  refers to the actual Earth’s mass.

## References

- Albarede F, Martine J. Unscrambling the lead model ages. *Geochimica et Cosmochimica Acta* 1984;48(1):207–12.
- Allègre CJ, Manhès G, Göpel C. The major differentiation of the earth at 4.45 ga. *Earth and Planetary Science Letters* 2008;267(1-2):386–98.
- Allègre CJ, Poirier JP, Humler E, Hofmann AW. The chemical composition of the earth. *Earth and Planetary Science Letters* 1995;134(3):515–26.
- Amelin Y. The u–pb systematics of angrite sahara 99555. *Geochimica et Cosmochimica Acta* 2008;72(19):4874–85.
- Barboni M, Boehnke P, Keller B, Kohl IE, Schoene B, Young ED, McKeegan KD. Early formation of the moon 4.51 billion years ago. *Science advances* 2017;3(1):e1602365.
- Bizzarro M, Baker JA, Haack H, Lundgaard KL. Rapid timescales for accretion and melting of differentiated planetesimals inferred from 26al-26mg chronometry. *The Astrophysical Journal Letters* 2005;632(1):L41.
- Boehnke P, Harrison TM. Illusory late heavy bombardments. *Proceedings of the National Academy of Sciences* 2016;113(39):10802–6.
- Bonsor A, Leinhardt ZM, Carter PJ, Elliott T, Walter MJ, Stewart ST. A collisional origin to earth’s non-chondritic composition? *Icarus* 2015;247:291–300.

- Borg LE, Connelly JN, Boyet M, Carlson RW. Chronological evidence that the moon is either young or did not have a global magma ocean. *Nature* 2011;477(7362):70.
- Boujibar A, Andraut D, Bolfan-Casanova N, Bouhifd MA, Monteux J. Cosmochemical fractionation by collisional erosion during the earth's accretion. *Nature communications* 2015;6.
- Bouvier A, Boyet M. Primitive solar system materials and earth share a common initial  $^{142}\text{Nd}$  abundance. *Nature* 2016;537(7620):399.
- Boyet M, Bouvier A, Frossard P, Hammouda T, Garçon M, Gannoun A. Enstatite chondrites  $\text{el}_3$  as building blocks for the earth: The debate over the  $^{146}\text{Sm}$ – $^{142}\text{Nd}$  systematics. *Earth and Planetary Science Letters* 2018;488:68–78.
- Boyet M, Carlson R.  $^{142}\text{Nd}$  evidence for early ( $> 4.53$  ga) global differentiation of the silicate earth. *Science* 2005;309(5734):576–81.
- Boyet M, Carlson RW, Borg LE, Horan M.  $\text{Sm}$ – $\text{Nd}$  systematics of lunar ferroan anorthositic suite rocks: constraints on lunar crust formation. *Geochimica et Cosmochimica Acta* 2015;148:203–18.
- Burkhardt C, Borg L, Brennecka G, Shollenberger Q, Dauphas N, Kleine T. A nucleosynthetic origin for the earth's anomalous  $^{142}\text{Nd}$  composition. *Nature* 2016;537(7620):394.
- Campbell IH, O'Neill HSC. Evidence against a chondritic earth. *Nature* 2012;483(7391):553.
- Carlson RW, Borg LE, Gaffney AM, Boyet M.  $\text{Rb}$ – $\text{Sr}$ ,  $\text{Sm}$ – $\text{Nd}$  and  $\text{Lu}$ – $\text{Hf}$  isotope systematics of the lunar  $\text{mg}$ –suite: the age of the lunar crust and its relation to the time of moon formation. *Philosophical Transactions of the Royal Society A: Mathematical, Physical and Engineering Sciences* 2014;372(2024):20130246.
- Carter PJ, Leinhardt ZM, Elliott T, Stewart ST, Walter MJ. Collisional stripping of planetary crusts. *Earth and Planetary Science Letters* 2018;484:276–86.
- Carter PJ, Leinhardt ZM, Elliott T, Walter MJ, Stewart ST. Compositional evolution during rocky protoplanet accretion. *The Astrophysical Journal* 2015;813(1):72.
- Carter PJ, Lock SJ, Stewart ST. The energy budgets of giant impacts. *Journal of Geophysical Research: Planets* 2020;125(1):e2019JE006042.
- Cartigny P, Boyd S, Harris J, Javoy M. Nitrogen isotopes in peridotitic diamonds from fuxian, china: the mantle signature. *Terra Nova* 1997;9(4):175–9.
- Chambers J, Wetherill G. Planets in the asteroid belt. *Meteoritics & Planetary Science* 2001;36(3):381–99.
- Chyba CF. Terrestrial mantle siderophiles and the lunar impact record. *Icarus* 1991;92(2):217–33.
- Clayton RN, Mayeda TK, Rubin AE. Oxygen isotopic compositions of enstatite chondrites and aubrites. *Journal of Geophysical Research: Solid Earth* 1984;89(S01):C245–9.
- Dauphas N. The isotopic nature of the earth's accreting material through time. *Nature* 2017;541(7638):521–4.
- Dauphas N, Davis AM, Marty B, Reisberg L. The cosmic molybdenum–ruthenium isotope correlation. *Earth and Planetary Science Letters* 2004;226(3–4):465–75.

- Dauphas N, Poitrasson F, Burkhardt C, Kobayashi H, Kurosawa K. Planetary and meteoritic mg/si and  $\delta^{30}\text{Si}$  variations inherited from solar nebula chemistry. *Earth and Planetary Science Letters* 2015;427:236–48.
- Drake MJ, Righter K. Determining the composition of the earth. *Nature* 2002;416(6876):39–44.
- Friedman A, Milsted J, Metta D, Henderson D, Lerner J, Harkness A, Op DR. Alpha decay half lives of 148gd 150gd and 146sm. *Radiochimica Acta* 1966;5(4):192–4.
- Halliday AN. The origins of volatiles in the terrestrial planets. *Geochimica et Cosmochimica Acta* 2013;105:146–71.
- Hartmann WK. History of the terminal cataclysm paradigm: Epistemology of a planetary bombardment that never (?) happened. *Geosciences* 2019;9(7):285.
- Holsapple KA, Housen KR. A crater and its ejecta: An interpretation of deep impact. *Icarus* 2007;191(2):586–97.
- Housen KR, Holsapple KA. Ejecta from impact craters. *Icarus* 2011;211(1):856–75.
- Jacobson SA, Morbidelli A. Lunar and terrestrial planet formation in the grand tack scenario. *Philosophical Transactions of the Royal Society A: Mathematical, Physical and Engineering Sciences* 2014;372(2024):20130174.
- Jacobson SA, Morbidelli A, Raymond SN, O’Brien DP, Walsh KJ, Rubie DC. Highly siderophile elements in earth’s mantle as a clock for the moon-forming impact. *Nature* 2014;508(7494):84.
- Javoy M. The integral enstatite chondrite model of the earth. *Geophysical Research Letters* 1995;22(16):2219–22.
- Javoy M, Kaminski E, Guyot F, Andraut D, Sanloup C, Moreira M, Labrosse S, Jambon A, Agrinier P, Davaille A, et al. The chemical composition of the earth: Enstatite chondrite models. *Earth and Planetary Science Letters* 2010;293(3-4):259–68.
- Javoy M, Pineau F. Stable isotope constraints on a model earth from a study of mantle nitrogen. *Meteoritics* 1983;18:320.
- Kinoshita N, Paul M, Kashiv Y, Collon P, Deibel C, DiGiovine B, Greene J, Henderson D, Jiang C, Marley S, et al. A shorter 146sm half-life measured and implications for 146sm-142nd chronology in the solar system. *Science* 2012;335(6076):1614–7.
- Kokubo E, Ida S. Formation of protoplanets from planetesimals in the solar nebula. *Icarus* 2000;143(1):15–27.
- Kruijer T, Touboul M, Fischer-Gödde M, Bermingham K, Walker R, Kleine T. Protracted core formation and rapid accretion of protoplanets. *Science* 2014;344(6188):1150–4.
- Leinhardt ZM, Dobinson J, Carter PJ, Lines S. Numerically predicted indirect signatures of terrestrial planet formation. *The Astrophysical Journal* 2015;806(1):23.
- Leinhardt ZM, Stewart ST. Collisions between gravity-dominated bodies. i. outcome regimes and scaling laws. *The Astrophysical Journal* 2011;745(1):79.

- Lugmair G, Shukolyukov A. Early solar system timescales according to 53mn-53cr systematics. *Geochimica et Cosmochimica Acta* 1998;62(16):2863–86.
- Manhes G, Allègre CJ, Dupré B, Hamelin B. Lead-lead systematics, the “age of the earth” and the chemical evolution of our planet in a new representation space. *Earth and Planetary Science Letters* 1979;44(1):91–104.
- Marcus RA, Stewart ST, Sasselov D, Hernquist L. Collisional stripping and disruption of super-earths. *The Astrophysical Journal Letters* 2009;700(2):L118.
- Masset F, Snellgrove M. Reversing type ii migration: resonance trapping of a lighter giant protoplanet. *Monthly Notices of the Royal Astronomical Society* 2001;320(4):L55–9.
- McDonough WF, Sun SS. The composition of the earth. *Chemical geology* 1995;120(3-4):223–53.
- Meissner F, Schmidt-Ott WD, Ziegeler L. Half-life and  $\alpha$ -ray energy of 146 sm. *Zeitschrift für Physik A Atomic Nuclei* 1987;327(2):171–4.
- Mojzsis SJ, Brasser R, Kelly NM, Abramov O, Werner SC. Onset of giant planet migration before 4480 million years ago. *The Astrophysical Journal* 2019;881(1):44.
- Morbidelli A, Crida A. The dynamics of jupiter and saturn in the gaseous protoplanetary disk. *icarus* 2007;191(1):158–71.
- Morbidelli A, Nesvorný D, Laurenz V, Marchi S, Rubie D, Elkins-Tanton L, Wieczorek M, Jacobson S. The timeline of the lunar bombardment: Revisited. *Icarus* 2018;305:262–76.
- Nakajima M, Stevenson DJ. Melting and mixing states of the earth’s mantle after the moon-forming impact. *Earth and Planetary Science Letters* 2015;427:286–95.
- Norman MD, Borg LE, Nyquist LE, Bogard DD. Chronology, geochemistry, and petrology of a ferroan noritic anorthosite clast from descartes breccia 67215: Clues to the age, origin, structure, and impact history of the lunar crust. *Meteoritics & Planetary Science* 2003;38(4):645–61.
- Nyquist L, Bogard D, Yamaguchi A, Shih CY, Karouji Y, Ebihara M, Reese Y, Garrison D, McKay G, Takeda H. Feldspathic clasts in yamato-86032: Remnants of the lunar crust with implications for its formation and impact history. *Geochimica et Cosmochimica Acta* 2006;70(24):5990–6015.
- O’Neill HSC, Palme H. Collisional erosion and the non-chondritic composition of the terrestrial planets. *Philosophical Transactions of the Royal Society of London A: Mathematical, Physical and Engineering Sciences* 2008;366(1883):4205–38.
- Pepin RO, Porcelli D. Xenon isotope systematics, giant impacts, and mantle degassing on the early earth. *Earth and Planetary Science Letters* 2006;250(3-4):470–85.
- Pierens A, Raymond SN. Two phase, inward-then-outward migration of jupiter and saturn in the gaseous solar nebula. *Astronomy & Astrophysics* 2011;533:A131.
- Raymond S, Kokubo E, Morbidelli A, Morishima R, Walsh K. Terrestrial planet formation at home and abroad. *Protostars and Planets VI* 2014;:595–618.
- Raymond SN, Izidoro A, Morbidelli A. Solar system formation in the context of extra-solar planets. *arXiv preprint arXiv:181201033* 2018;.

- Raymond SN, Morbidelli A. The grand tack model: a critical review. *Proceedings of the International Astronomical Union* 2014;9(S310):194–203.
- Raymond SN, O’Brien DP, Morbidelli A, Kaib NA. Building the terrestrial planets: constrained accretion in the inner solar system. *Icarus* 2009;203(2):644–62.
- Raymond SN, Quinn T, Lunine JJ. High-resolution simulations of the final assembly of earth-like planets i. terrestrial accretion and dynamics. *Icarus* 2006;183(2):265–82.
- Ringwood AE. The chemical composition and origin of the earth. In: *Advances in earth science*. volume 65; 1966. p. 287.
- Ruzicka A, Snyder GA, Taylor LA. Vesta as the howardite, eucrite and diogenite parent body: Implications for the size of a core and for large-scale differentiation. *Meteoritics & Planetary Science* 1997;32(6):825–40.
- Shibaike Y, Sasaki T, Ida S. Excavation and melting of the hadean continental crust by late heavy bombardment. *Icarus* 2016;266:189–203.
- Shuvalov V. Atmospheric erosion induced by oblique impacts. *Meteoritics & Planetary Science* 2009;44(8):1095–105.
- Srinivasan G, Goswami J, Bhandari N. 26Al in eucrite piplia kalan: Plausible heat source and formation chronology. *Science* 1999;284(5418):1348–50.
- Svetsov V. Cratering erosion of planetary embryos. *Icarus* 2011;214(1):316–26.
- Tanaka H, Inaba S, Nakazawa K. Steady-state size distribution for the self-similar collision cascade. *Icarus* 1996;123(2):450–5.
- Thiemens MM, Sprung P, Fonseca RO, Leitzke FP, Münker C. Early moon formation inferred from hafnium–tungsten systematics. *Nature Geoscience* 2019;12(9):696–700.
- Touboul M, Kleine T, Bourdon B, Palme H, Wieler R. Late formation and prolonged differentiation of the moon inferred from W isotopes in lunar metals. *Nature* 2007;450(7173):1206.
- Touboul M, Kleine T, Bourdon B, Palme H, Wieler R. Tungsten isotopes in ferroan anorthosites: Implications for the age of the moon and lifetime of its magma ocean. *Icarus* 2009;199(2):245–9.
- Touboul M, Puchtel IS, Walker RJ. 182W evidence for long-term preservation of early mantle differentiation products. *science* 2012;335(6072):1065–9.
- Touboul M, Puchtel IS, Walker RJ. Tungsten isotopic evidence for disproportional late accretion to the earth and moon. *Nature* 2015;520(7548):530.
- Walker RJ. Highly siderophile elements in the earth, moon and mars: update and implications for planetary accretion and differentiation. *Chemie der Erde-Geochemistry* 2009;69(2):101–25.
- Walsh KJ, Morbidelli A, Raymond SN, O’Brien DP, Mandell AM. A low mass for mars from jupiter’s early gas-driven migration. *Nature* 2011;475(7355):206.
- Warren PH. Stable-isotopic anomalies and the accretionary assemblage of the earth and mars: A subordinate role for carbonaceous chondrites. *Earth and Planetary Science Letters* 2011;311(1–2):93–100.

- Weidenschilling S. The distribution of mass in the planetary system and solar nebula. *Astrophysics and Space Science* 1977;51(1):153–8.
- Wetherill G. The formation and habitability of extra-solar planets. *Icarus* 1996;119(1):219–38.
- Wetherill GW. Accumulation of the terrestrial planets. *prpl* 1978;:565.
- Wetherill GW. Occurrence of giant impacts during the growth of the terrestrial planets. *Science* 1985;228(4701):877–9.
- Wetherill GW. Formation of the earth. *Annual Review of Earth and Planetary Sciences* 1990;18(1):205–56.
- Wetherill GW. An alternative model for the formation of the asteroids. *Icarus* 1992;100(2):307–25.
- Workman RK, Hart SR. Major and trace element composition of the depleted morib mantle (dmm). *Earth and Planetary Science Letters* 2005;231(1):53–72.
- Yamaguchi A, Taylor GJ, Keil K. Metamorphic history of the eucritic crust of 4 vesta. *Journal of Geophysical Research: Planets* 1997;102(E6):13381–6.
- Zellner NE. Cataclysm no more: new views on the timing and delivery of lunar impactors. *Origins of Life and Evolution of Biospheres* 2017;47(3):261–80.

## Appendice

### 4.1. Influence of the partial melting rate

When forming a new crust, the mantle partial melting rate is determinant for the repartition of the chemical elements between crust and mantle. As it is evidenced in the eq.1, the higher the partial melting rate  $f_{p-c}^1$ , the lower the concentration in Nd within the crust. As a consequence, the preferential loss of Nd compared to Sm is lower for a higher partial melting rate. A given amount of eroded crust leads to a lower fractionation in the Sm/Nd ratio for a higher  $f_{p-c}^1$ . The results for three different partial melting rates are presented in fig.4. This parameter clearly has a non neglectable influence on the final results; however, since when it increases the fractionation decreases. Accordingly,  $f_{p-c}^1$  has been chosen low (2.6%) to estimate an upper bound of possible impact-induced fractionation.

### 4.2. Influence of the Size-frequency distribution

The final results concerning the evolution of the fractionation value ( $\epsilon$ ) over time have been computed for 3 other  $\alpha$ : 2.5, 3 and 4.1. As the concern is only the influence of the slope over the fractionation, we present it only for the different classical simulations, that in average, produce a higher fractionation value than the Grand Tack scenario. They are presented in fig. 5. The solid colored lines represent the results presented above (with  $\alpha = 3.5$ ), the dashed lines represents the results of the three different mixing scenarios for  $\alpha = 2.5$  and the last represents the results for  $\alpha = 4.1$ . The higher  $\alpha$  (i.e. more mass in the smaller bodies), the lower  $\epsilon$ . It may be expected that earlier in the planetary formation history, the slope would have been slightly higher (Tanaka et al., 1996). As a consequence, the fractionation estimated in this study could be overestimated. However, the difference between the different models from different  $\alpha$  are very low, so the choice of this parameter is not critical.

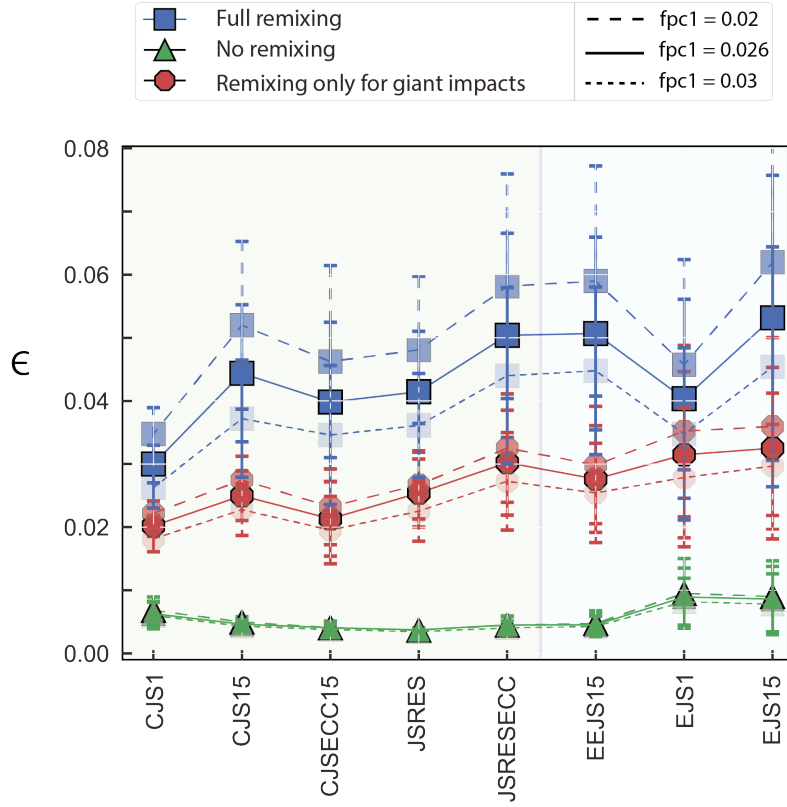


Figure 4: Partial melting rate influence on the final embryos fractionation evidenced by representation of  $\epsilon$  mean values for the different dynamical scenarios in a classical accretion disk. Solid lines represent the model presented in the main text while dashed lines represent the results for other  $\alpha$  tested here. The colors and markers refer to the mixing scenarios.

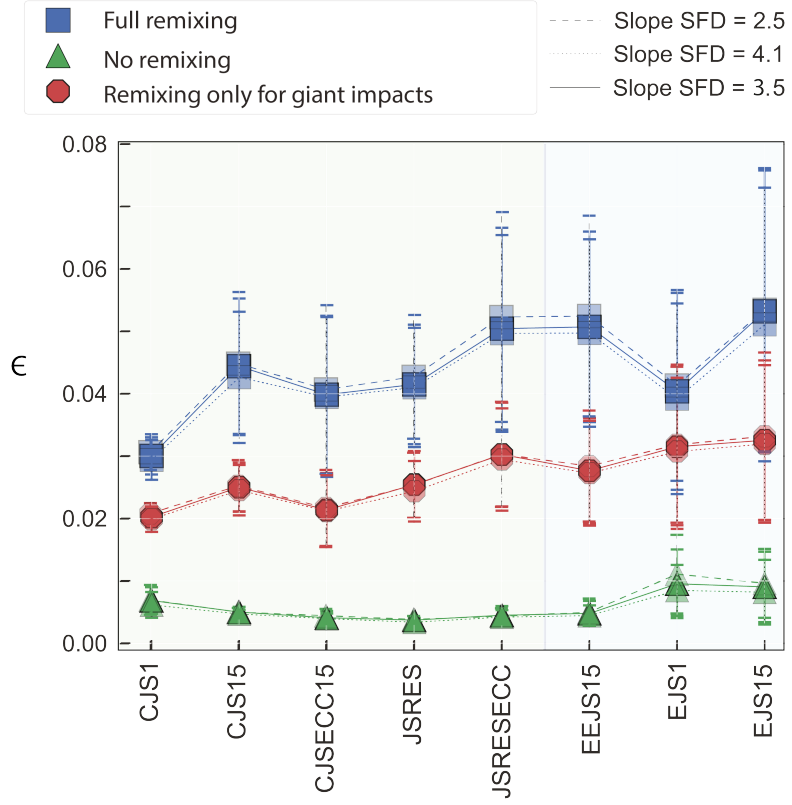


Figure 5:  $\alpha$  (SFD slope) influence on the final embryos fractionation evidenced by representation of  $\epsilon$  mean values for the different dynamical scenarios. Solid lines represent the model presented in the main text while dashed lines represent the results for other  $\alpha$  tested here. The colors and markers refer to the mixing scenarios.



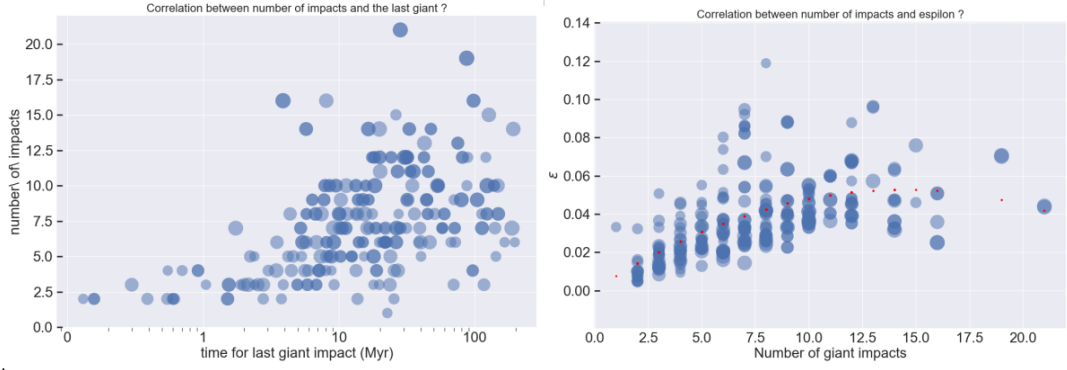


Figure 6: (1) Left panel. Number of impacts suffered by the embryos surviving to Grand Tack simulations as a function of the timing for the last giant impact. (2) Right panel.  $\epsilon$  value for epsilon as a function of the number of giant impacts for Grand-Tack surviving embryos. In both figures the sizes of the circles stand the final masses of the surviving embryo.

#### 4.3. Correlation with the last giant impact is not due to the number of giant impacts

Figure 6 shows 1) on the left panel the number of impacts suffered by the embryos surviving to Grand Tack simulations as a function of the timing for the last giant impact; and 2) on the right panel, the epsilon value for epsilon as a function of the number of giant impacts for Grand-Tack surviving embryos. We see no correlation between any of these values. The only thing that can be pointed out by this figure is the dispersion after a few Myr that becomes extremely large. This denotes the fact that the correlation observed for the Grand Tack scenario between the fractionation of the Earth analogs and the time they registered their last involvement into a giant impact is not linked to the number of giant impacts they went through. The correlation is a correlation to the timing of the last chemical re-equilibration and not on how often a re-equilibration has occurred.

#### 4.4. Influence of the choice for the cratering model

The scaling laws for rocky targets (Holsapple and Housen, 2007) has been chosen when integrated over all impact angles (Svetsov, 2011) for the description of the eroded mass. However, Svetsov (2011) explores and improves an other scaling law that has been suggested (Shuvalov, 2009) based on simulations of impacts in the presence of planetary atmospheres. This very last description is tested in this study, to explore the influence that could have the choice of the cratering model used. This formulation of eroded mass is described before discussing the associated results.

The escaped mass is estimated as Svetsov (2011):

$$M_{escaped} = m_{imp} C(V_{imp}) \frac{V_{imp}^2 - C_1(V_{imp}) v_{esc}^2}{v_{esc}^2} \left( \frac{V_{imp}}{20 v_{esc}} \right)^a, \quad (8)$$

with  $m_{imp}$  and  $V_{imp}$  being respectively the impactor mass and the impact velocity. Here,  $v_{esc}$  is assumed to be the two-body escape speed:

$$v_{esc} = \sqrt{\left( \frac{2G(m_{tar} + m_{imp})}{R_{tar} + R_{imp}} \right)}, \quad (9)$$

with  $m_{tar}$  the target mass,  $R_{tar}$  and  $R_{imp}$  are respectively the target and the impactor radius. The different dimensionless coefficients needed for the calculation of  $M_{escaped}$ , are defined as follows:

$$C_1(V_{imp}) = 0.7 + (V_{imp}/20 \text{ km/s})^2, \quad (10)$$

$$a = 0.15 - 0.0003(V_{imp} - 15 \text{ km/s})^2, \quad (11)$$

And, concerning  $C$  (wich is also a dimensionless number):

- if  $V_{imp} \geq 20 \text{ km/s}$ , then  $C(V_{imp}) = 0.02$ ,
- if  $V_{imp} = 10 \text{ km/s}$ , then  $C(V_{imp}) = 0.035$ ,
- if  $V_{imp} \leq 5 \text{ km/s}$ , then  $C(V_{imp}) = 0.07$ ,
- if  $5 \text{ km/s} < V_{imp} < 10 \text{ km/s}$ , then  $C(V_{imp}) = 0.07 + [(0.035 - 0.07)/5](V_{imp} - 5)$ ,
- if  $10 \text{ km/s} < V_{imp} < 20 \text{ km/s}$ , then  $C(V_{imp}) = 0.02 + [(0.02 - 0.035)/10](V_{imp} - 10)$ .

The two different scaling laws are tested over all the collisional histories of the different embryos issued from the numerical simulations. Depending on the range of impact velocity, either one model overestimates the escaped mass compared to the other, either it underestimates it. However, the difference between the two different models is not critical. For both models the final  $\epsilon$  values are similar within a few percents and show a  $\epsilon$  below 0.05.

#### 4.5. Three sets of assumptions for mass balance modeling

We present here the description of the two additional mixing scenarios for chemical mass balance resulting from impacts. These are end-members meant to provide lower-bound and maximum-bound fractionation.

##### 4.5.1. Scenario 1: "the full remixing" model

The BSP is molten and the newly formed crust reequilibrates with the mantle after each impact. Giant impacts are considered as perfect mergers, and a full reequilibration between crust and mantle is still assumed. Expressions 1 and 2 are used for estimating the resulting BSP concentration in a given element  $M$  compared to its previous value.

##### 4.5.2. Scenario 2: "no remixing" model

Only small impacts are taken into account for estimating the masses of eroded crust and accreted chondritic material. All accreted material is assumed to fall onto the surface so that only the crustal composition is modified while mantle composition (and its mass) remains constant. No new crust is formed. Accordingly, the new composition of the crust in  $M$  at a given time  $i$  is expressed following:

$$C_{Mcrust}^i = \frac{C_{Mcrust}^{i-1} m_{crust}^{i-1} + C_M^{chondritic} m_{accreted}^i - C_{Mcrust}^{i-1} m_{ejected}^i}{m_{crust}^{i-1} + m_{accreted}^i - m_{ejected}^i}, \quad (12)$$

where  $m_{crust}$  is the crustal mass,  $C_M^{chondritic}$  is the chondritic concentration for the element  $M$ ,  $m_{accreted}$  is the accreted mass (from impactor) and  $m_{ejected}$  is the escaped mass.

In this scenario, the giant impacts are not treated at all in terms of mass balance. It means that when a giant impact is recorded into N-body collisions file, our model is ignoring it, it behaves exactly as if proto-Earth remained perfectly intact. No new crust is formed from partial melting. It is far from realistic scenario, but is meant to represent a end-members.

The scenario 1 (full remixing) and 2 (no remixing) represent unrealistic end members. As a consequence, previously, only the most realistic case, the scenario 3 (remixing only for giant impacts) has been presented. The results concerning the other two cases are presented here in details (7 and 8). The values of  $\epsilon$  range from  $0.029 \pm 0.003$  to  $0.05 \pm 0.02$  for the classical scenario in the case of the mixing scenario (1) (fig. 7) which is clearly the most favorable to fractionate the Sm/Nd ratio with respect to chondritic composition. In this case, a new crust is formed after each impact and Sm and Nd are re-distributed according to their partition coefficients between the solid mantle and the liquid crust. This leads to an increase of the Nd/Sm ratio of the newly formed crust at each step of the simulation as Nd is more incompatible than Sm. However, this scenario is not appropriate as low energy events are not likely to produce large amounts of melt and can be consider as an upper bound for the final modeled Sm/Nd ratio of the bulk silicate Earth. In the case of the mixing scenario (2) (fig. 8,  $\epsilon$  takes values between  $0.0037 \pm 0.0004$  and  $0.009 \pm 0.006$  for a classical accretion scenario. In this scenario the crust is refertilized in chondritic Sm/Nd after each impact and absence of melting leads to the lowest chemical fractionation of the Sm/Nd value. The crust mass increases and becomes more and more chondritic during the course of accretion. This scenario can be considered as the opposite as scenario 1, and provides a lower bound for  $\epsilon$  values. The global trend of those observation is found also concerning the grand tack simulations. However, the final fractionation values are much more spread out. Especially, concerning the most favorable case to fractionation: full remixing; the values of the  $\epsilon$  fractionation are very high in average ( $0.12 \pm 0.03$ ). Such fractionation is unexpected as we do not sample any extraterrestrial body or meteorite that would present such values of Sm/Nd ratio. However, since the grand tack has a powerful effect of fractionation during the first Myrs of accretion, is the crust is enriched in Nd at each step because of a new crust-forming event due to complete melting of the silicate Earth, it is clear that the total fractionation will take unrealistically large values. As a conclusion, those two end members gives us clues about the very lower and upper bound of the fractionation, but they still quite unrealistic and they are not strong enough to allow a better approach and constrain the Sm/Nd ratio evolution over accretion histories. That is the reason why the intermediate case (3) - remixing only for giant impacts - has been chosen alone to follow this fractionation. It provides a good first approximation of the fractionation as a response to collisional erosion.

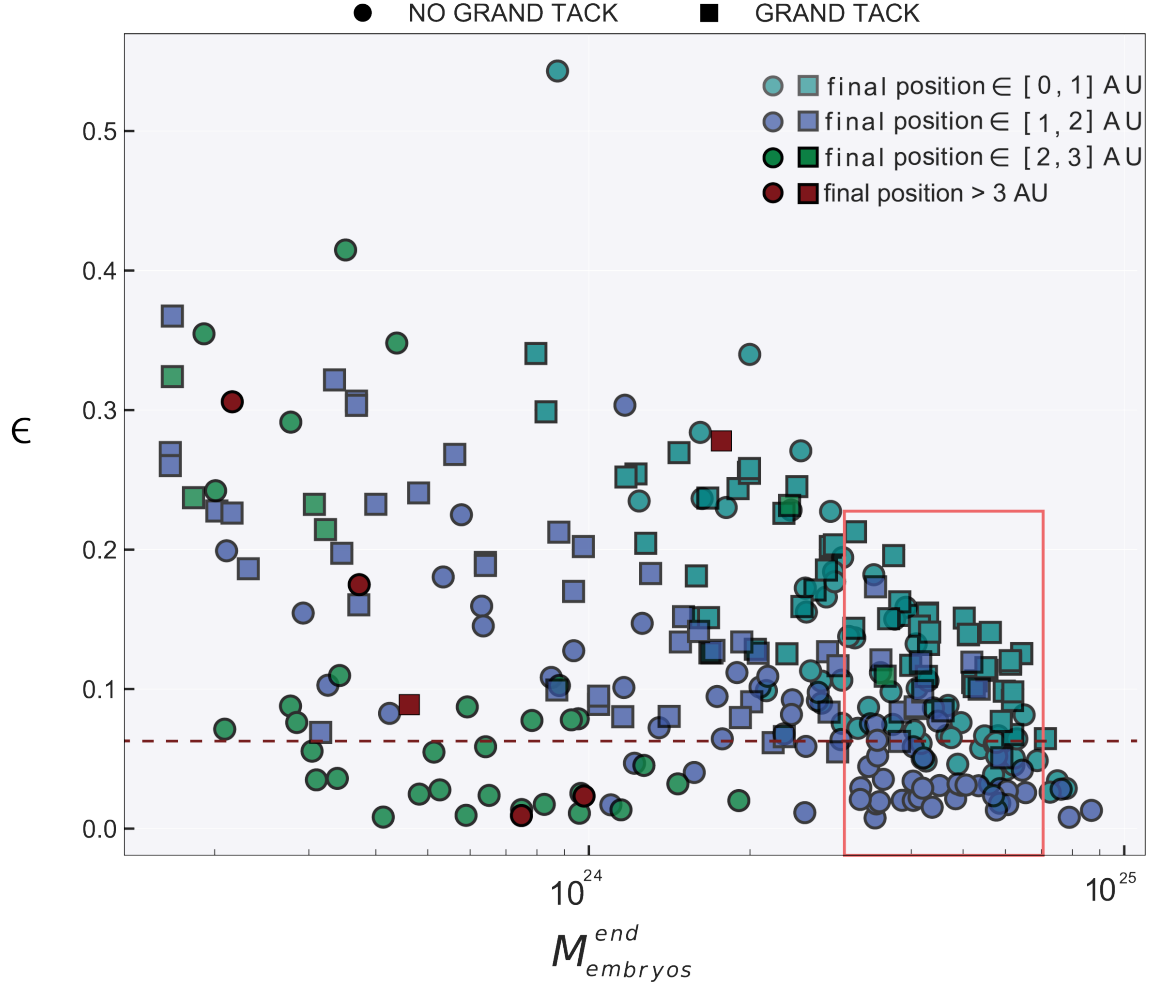


Figure 7:  $\epsilon$  (Sm-Nd fractionation) with respect to chondritic Sm/Nd values of the different surviving embryos at the end of classical and Grand Tack N-body simulations reported as a function of their final masses. The remixing model adopted here is the most favorable to fractionation (scenario 1: full remixing). The markers refer to the type of accretionary scenario (circles for the classical scenario and square for grand tack). The colors refer to the final semi-major axis of the embryos. The red box shows the Earth analogs.

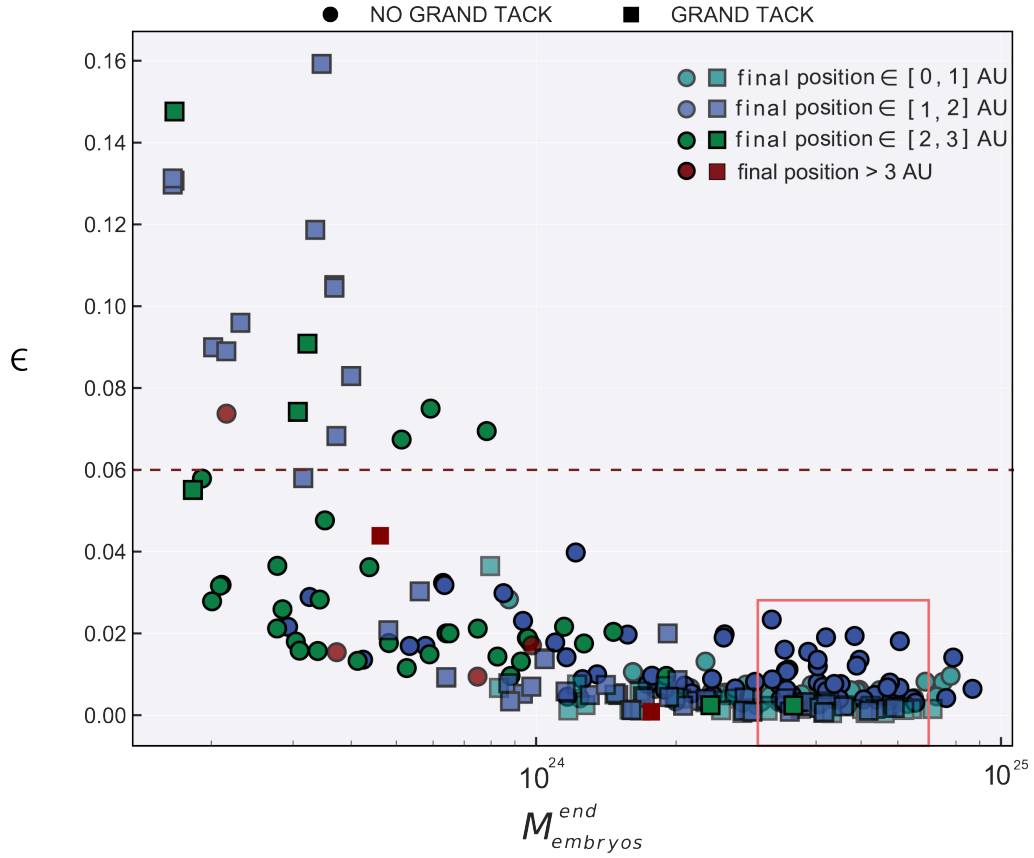


Figure 8:  $\epsilon$  (Sm-Nd fractionation) with respect to chondritic Sm/Nd values of the different surviving embryos at the end of classical and Grand Tack N-body simulations reported as a function of their final masses. The remixing model adopted here is the less favorable to fractionation (scenario 2: no remixing). The markers refer to the type of accretionary scenario (circles for the classical scenario and square for grand tack). The colors refer to the final semi-major axis of the embryos. The red box shows the Earth analogs.